

STRUCTURAL CHARACTERIZATION AND COMPRESSIVE BEHAVIOR OF THE BOXFISH HORN

Wen Yang^{1*}, Vanessa Nguyen², Michael M. Porter¹, Marc A. Meyers^{1,2,3}, Joanna McKittrick^{1,2}

¹Materials Science and Engineering Program, ²Department of Mechanical and Aerospace Engineering, ³Department of Nanoengineering

University of California, San Diego, La Jolla, CA 92093, USA

* Corresponding author, email: wey005@eng.ucsd.edu

ABSTRACT

Boxfish have a rigid carapace that restricts body movement making them slow swimmers. Some species of boxfish (*Lactoria cornuta*) have lightweight horns that function as a form of defense. The boxfish horns are nearly hollow and have an intricate hierarchical structure. The structural organization and compressive properties of the boxfish horns are described here to understand the mechanical behavior and damage mechanisms.

INTRODUCTION

Boxfish, belonging to the family *Ostraciidae*, are named after their unique boxy profile, which is generally an oblong, triangular or square-like shape. There are over twenty species of fish in the family *Ostraciidae*, which live in the Atlantic, Pacific and Indian Oceans [1,2]. Found in warm tropical and subtropical waters, they typically inhabit coral reefs and grass beds at depths of 1 to 45 m [3]. They are usually yellow; however, their color can vary, ranging from orange, green, blue or white [4]. They also secrete toxins into the surrounding water to deter predators [5]. Their body, growing up to 50 cm in length, is composed of a rigid carapace that restricts significant body movement [6-8]. The carapace is composed of several highly mineralized [9], hexagonal dermal scutes (bony plates), with some incidence of heptagons and pentagons (shown in Figure 1a). As a result, they are relatively slow swimmers that glide or hover through the water - a method of locomotion known as ostraciiform swimming [10]. The boxy shape and rigid carapace allow the boxfish to swim in this manner by minimizing vortices and drag [8].

One species, *Lactoria cornuta*, is called the longhorn cowfish because of the two long horns that protrude from the head. Another pair of horns are located below the caudal fin and protrude from the posterior. Khan et al. [11] suggested that the horns are a type of defense mechanism, providing obstructions that discourage other fish from swallowing them. They also state that the horns can be regenerated in a few months if broken off, indicating the horns are a necessary adaptation developed for protection from predators.

The boxfish scutes and fish scales are composed of hydroxyapatite ($\text{Ca}_{10}(\text{PO}_4)_6(\text{OH})_2$) and type I collagen [9, 12, 13]. Similarly, the horns should also be composed of mineralized collagen fibers. The arrangement of the mineralized fibers significantly affects the mechanical properties in bony tissues [14].

The purpose of this work is to analyze the mechanical properties and structure of the boxfish horns. Understanding the mechanical behavior and damage mechanisms of these horns may provide inspiration for lightweight synthetic materials for structural or defense applications.

EXPERIMENTAL TECHNIQUES

Two boxfish (deceased), *Lactoria cornuta*, were obtained from Scripps Institution of Oceanography at University of California, San Diego and preserved in 70% isopropanol. The

structure of the boxfish horns was examined by 3D digital optical microscopy, scanning electron microscopy (SEM), and micro-computed tomography (μ -CT). The compressive mechanical properties and fracture mechanisms were investigated by compressing a small section of a single horn.

A whole boxfish, including its horns, was scanned with a Skyscan 1076 (Kontich, Belgium) μ -CT scanner. For sample preparation, the boxfish was wrapped in tissue paper moistened with a phosphate buffer saline solution and placed in a sealed tube to prevent the specimen from drying out during scanning. An isotropic voxel size of 36 μ m, an electric potential of 100kV, and a current of 100 μ A was applied during scanning using a 0.5 mm aluminum filter with a rotation step of 0.6 degrees and exposure time of 90 ms. A beam hardening correction algorithm was applied during image reconstruction. Images and 3D rendered models were analyzed using Skyscan's Data Viewer and CTVOx software.

To characterize the structure, two sections of the horn were cut - one along the longitudinal direction and one in the transverse (cross-sectional) direction. Both sections were partially deproteinized in a 6% NaClO solution for 15 min to better visualize the microstructures [15]. The partially deproteinized horn sections were observed with a digital optical microscope (VHX-1000, Keyence, NJ) and environmental scanning electron microscope (FEI-XL30, FEI Company, Hillsboro, OR). Before SEM observation, the horn sections were fixed in a 2.5% glutaraldehyde solution for 3 hrs, then immersed in a gradient ethanol series (30 vol.%, 50 vol.%, 75 vol.%, 80 vol.%, 95 vol.% to 100 vol.%) to remove water from the specimens while preventing shrinkage due to dehydration. The samples immersed in ethanol were dried in a critical point dryer (Auto Samdri 815A, Tousimis, MD) to preserve the original shape of the horns. The dried samples were then sputter coated with iridium using an Emitech K575X sputter coater (Quorum Technologies Ltd., West Sussex, UK) and examined by SEM.

A small section (1.5 mm in length) of a horn was cut and loaded in compression using a load frame (Instron 3342, Norwood, MA). The diameter of the sample gradually decreased from the root to the tip, from \sim 1.75 mm to \sim 1.6 mm. As the sample was short, no attachments were fixed on the sample. The sample was immediately tested after removal from the isopropanol and loaded longitudinally with a strain rate of 10^{-3} sec^{-1} .

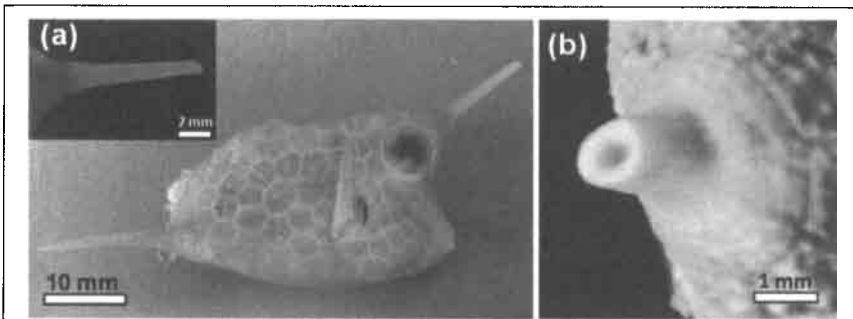


Figure 1. (a) Photograph of the dextral view of a boxfish (*Lactoria cornuta*) and one horn (top left); (b) micro-computed tomography image showing the transverse cross-section of a horn.

STRUCTURAL CHARACTERIZATION OF THE BOXFISH HORN

Figure 1a shows the dextral side of the boxfish. The length of the whole boxfish, including the horns and tail, is ~60 mm. The horns of the fish are ~12 mm long and appear hollow in the μ -CT image (Figure 1b), which demonstrates that the horn sheath is mineralized.

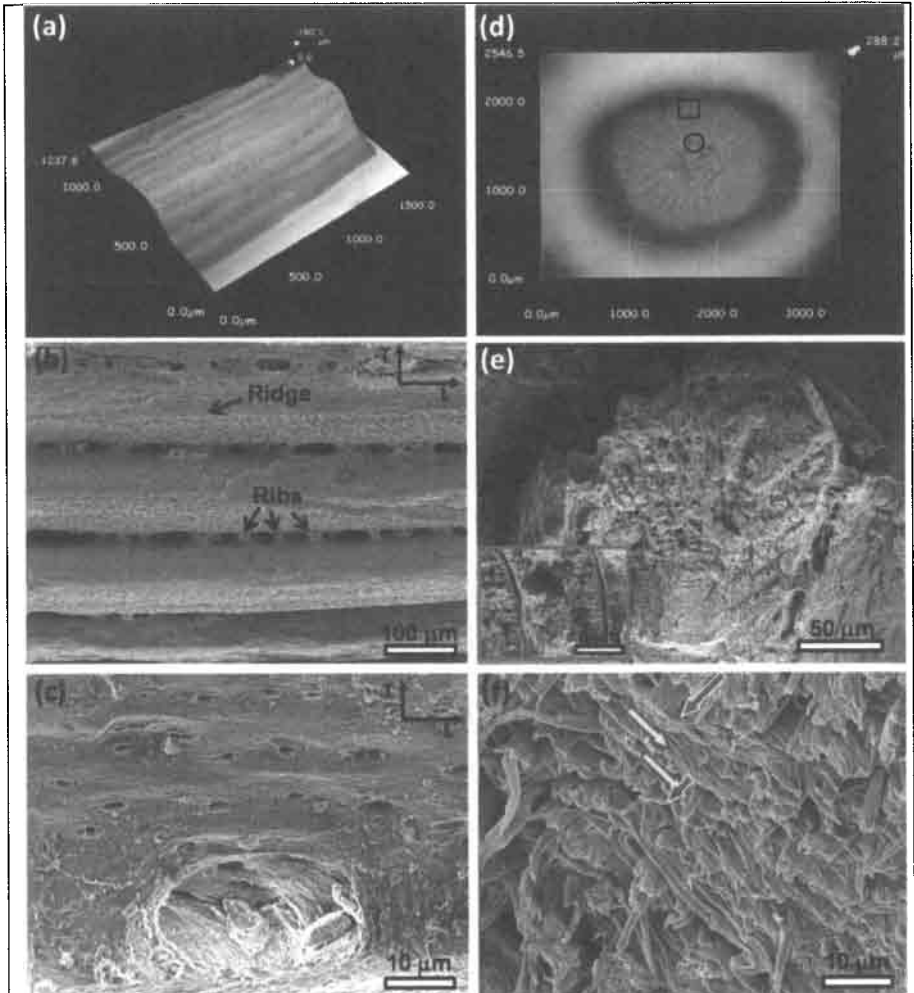


Figure 2. Images of the outer and inner surfaces of the horn. (a) 3D digital microscopic image of the partially deproteinized outer surface showing a petal-like feature composed of ridges; (b) SEM image showing ribs connecting the ridges (L and T in the coordinate system represents the longitudinal and transverse directions, respectively); (c) SEM image of small pores on the outer surface; (d) 3D digital microscopic image of the transverse cross-section; (e) SEM images of fibers extending through the petal-like feature similar to the veins of a leaf from the square region in (d); (f) SEM image of the cross-fiber pattern from circle region in (d).

Figure 2 shows the structural hierarchy of a selected region in the middle of a partially deproteinized horn. The outer surface is composed of several arch-like ridges oriented in the longitudinal direction (Figure 2a). The average diameter of each ridge is $\sim 100 \mu\text{m}$ (Figure 2b). Between the longitudinal ridges are perpendicularly oriented fibers (ribs) that connect adjacent ridges with a spacing of $10\text{-}100 \mu\text{m}$ (Figure 2b). The ridge surfaces contain several small pores $\sim 3 \mu\text{m}$ in diameter (Figure 2c). Figure 2d shows the horn cross-section. The outer and inner diameters are 1.8 and 0.8 mm , respectively. The edges of each ridge (see Figures 2a and 2b) extend from the outer surface towards the center, creating a ribbed structure that resembles the petals of a flower. The central core is filled with a low-density organic network near the base (Figure 2d). Figure 2e shows higher magnification of the outer edge of a single rib (square in Figure 2d). The fibers extend through the structure from the center to the edge with $\sim 10 \mu\text{m}$ spacing between fiber bundles (left bottom image in Figure 2e). Figure 2f shows higher magnification of the inner edge of a single rib (circle in Figure 2d), which has two orientations of fibers that are perpendicular to each other. These hierarchical structures appear to make the horns lightweight and rigid.

The density of the central matrix of the horn decreases from the base to the tip. Figure 3a shows across-section of the horn $\sim 3\text{mm}$ from the tip. It is clear that the central region is nearly hollow. The ribbed units contain 2-5 tubules aligned in the longitudinal direction. The fibers appear to be aligned circumferentially around the pores/tubules, as shown in Figure 3b. The average diameter of the tubules changes from $44 \mu\text{m}$ (close to core) to $18 \mu\text{m}$ (close to periphery). This gradation in pore diameter has been observed in the foam structure of porcupine quill [16] and channels in the structure of sucker rings from *Dosidicus gigas* [17]. Although the horn is mineralized, due to the extensive porosity, the overall density (by weight and dimension measurements) is $\sim 1000 \text{ kg/m}^3$. Nature creates larger tubules/channels/cells in the center to reduce the density but maintain bending resistance. The center of a cylinder does not experience substantial bending stress, thus the material can be removed without compromising the bending resistance. Although bending tests would enhance the analytical results, in this work, due to the limited number of horns and the small sample size, these tests were not performed. However, this unidirectional alignment indicates that the boxfish horn should be stronger when loaded in the longitudinal direction than in other directions [13].

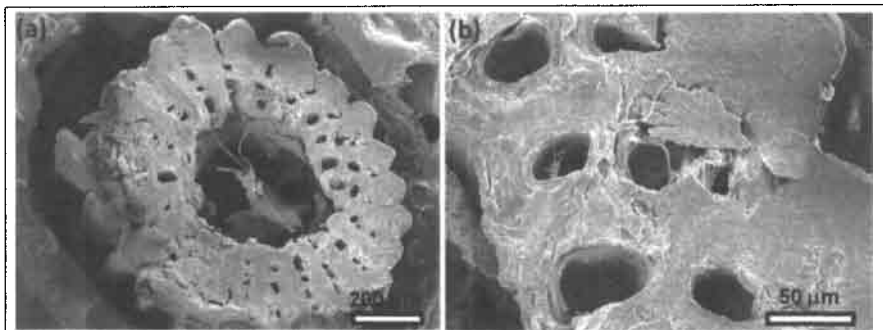


Figure 3. (a) Cross-section of horn close to the tip, (b) several tubules running longitudinally through the horn.

COMPRESSIVE BEHAVIOR AND DAMAGE MECHANISMS

Since the boxfish horn is used for protection and defense, it may be subjected to compressive loading. Therefore, a small section of the horn was selected to investigate the compressive behavior and evaluate the damage mechanisms. An image of this section is shown in Figure 4. The stress-strain curve (Figure 4) was calculated assuming the horn is a hollow cylinder with a wall thickness of ~ 500 μm . For this sample, the stiffness of the horn is ~ 430 MPa and the failure strength is ~ 80 MPa at a strain of $\sim 30\%$. The horn demonstrated high toughness, as evidence by the considerable plastic deformation experienced before failure, which may involve multiple deformation modes.

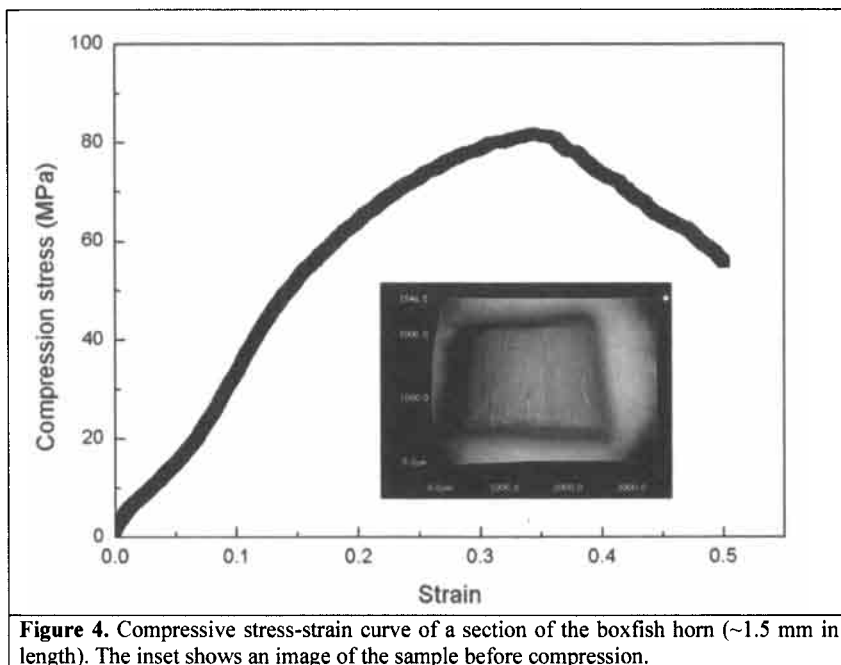


Figure 4. Compressive stress-strain curve of a section of the boxfish horn (~ 1.5 mm in length). The inset shows an image of the sample before compression.

After compression testing, the fracture surfaces were examined by SEM. The sample fractured between the ridges, as shown in Figure 5a. Some of the ridges buckled (arrow in Figure 5a). At the fractured edges, large fiber bundles pulled out, revealing more clearly the thin fibers connecting the bundles to the matrix (arrows in Figure 5b). Before fracture, most of the fibers showed considerable plastic deformation in the form of necking (arrows in Figure 5c). The fiber bundles also underwent delamination (square in Figure 5d) and buckling (arrow in Figure 5d). As the spacing between ridges deformed, the network of fibers connecting them (ribs) remained mostly intact. All these mechanisms contribute to high energy absorption under compressive loading, providing the horn the necessary toughness to function as a protective appendage.

In summary, the density of the pores/tubules in the boxfish horn decreases from the core to the periphery. As shown in Figure 3, it is believed that the fibers are aligned circumferentially around the pores in the structure. The alignment of the tubules most likely makes the boxfish

horn stronger in the longitudinal directions compared to the other orthogonal directions[13]. Compared to the compressive strength of bovine cortical bone (150~180 MPa) the boxfish horn is about half (~ 80 MPa) in the longitudinal direction. However, the density of boxfish horn (1000 kg/m³) is lower than that of bovine cortical bone (2100 kg/m³)[19], therefore the strength per unit weight of the boxfish horn is almost the same as cortical bone. The high strength per unit weight results from other structure features. The horn has ribs in the circumferential direction that connect the ridges, and under loading the ribs remain intact to retain structural integrity. Thus, the architecture of the boxfish horn is a model for biomimetic/bioinspired materials design, as it possesses low density, high strength and high toughness.

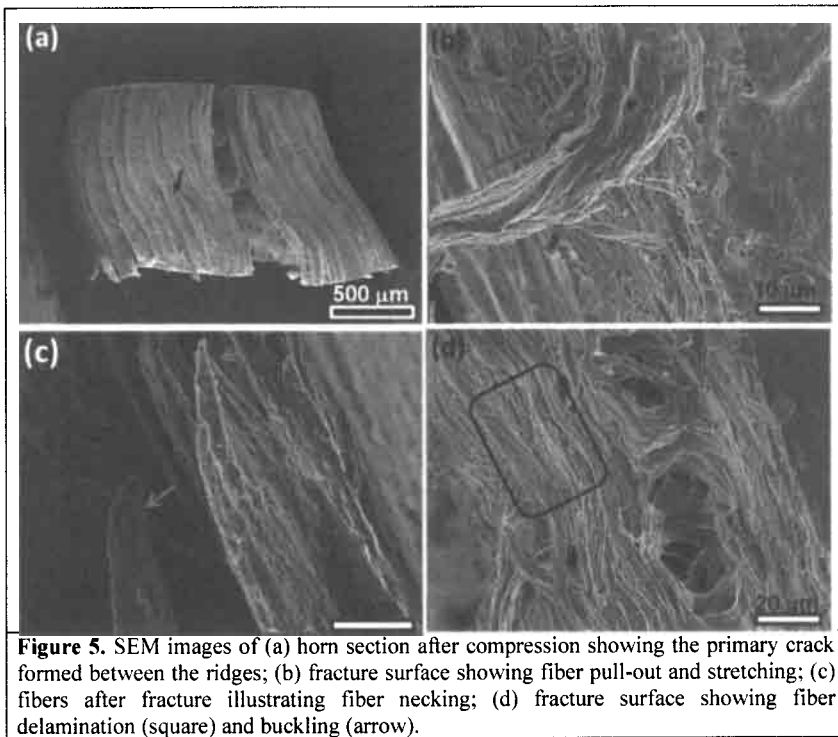


Figure 5. SEM images of (a) horn section after compression showing the primary crack formed between the ridges; (b) fracture surface showing fiber pull-out and stretching; (c) fibers after fracture illustrating fiber necking; (d) fracture surface showing fiber delamination (square) and buckling (arrow).

CONCLUSIONS

This study reports on the structural characterization, compression behavior, and damage mechanisms of the boxfish (*Lactoria cornuta*) horn, which are reviewed as follows:

1. The horn is composed of a mineralized conical sheath that has an organic network inclusion. The density of the organic inclusion decreases from the base to the tip of the horn, becoming nearly hollow.
2. The sheath, which provides most of the horn support, has a hierarchical structure. It has several petal-shaped units on the outer surface that are composed of ridges. The ridges are connected by ribs oriented roughly perpendicular to the ridges. Each ribbed unit is

composed of fibers that extend from the center core to the outer surface. Small tubules (10-50 μm) run longitudinally through the outer sheath.

3. The compressive strength of the horn is ~80 MPa at a failure strain of ~30%.
4. Under compressive loading, longitudinally oriented fibers delaminate, buckle, and neck before fracture, demonstrating that the horn has an energy dissipative structure.
5. The horn has a similar compressive strength to weight ratio as bovine cortical bone.

ACKNOWLEDGEMENTS

We thank Prof. Phil Hastings and H.J. Walker at the Scripps Institute of Oceanography for providing the boxfish. Prof. Robert Sah and Esther Cory are thanked for performing and helping interpret the micro-computed tomography. This work is supported by the National Science Foundation, Ceramics Program Grant 1006931 and UC Lab Research Program, 09-LR-06-118456-MEYM.

REFERENCES

1. F. Santini, L. Sorenson, T. Marcroft, A. Dornburg and M.E. Alfaro, "A multilocus molecular phylogeny of boxfishes (Aracanidae, Ostraciidae; Tetraodontiformes)," *Mol. Phylogenet. Evol.*, **66**, 153-160 (2013).
2. M.A. Ambak, M.M. Isa, M.Z. Zakaria, and M.B. Ghaffar, *Fishes of Malaysia*, 1st Ed., Terengganu: University Malaysia Terengganu Press (2010).
3. J.B. Hutchins, Ostraciidae. In FAO species identification sheets for fishery purposes. Western Indian Ocean (Fishing area 51), Vol. 3, edited by W. Fischer and G. Bianchi, 9. Rome: FAO (1984).
4. <http://marinebio.org/species.asp?id=1463> Longhorn Cowfishes, *Lactoria cornuta*, 14 January 2013.
5. K. Tachibana, "Chemical defense in fish," in *Bioorganic Marine Chemistry*, P.J. Scheuer, Ed., **2**, 117-138 (1988).
6. J.R. Hove, L.M. O'Bryan, M.S. Gordon, P.W. Webb and D. Weihs, "Boxfishes (Teleostei: Ostraciidae) as a model system for fishes swimming with many fins: kinematics," *J. Exp. Biol.*, **204**, 1459-1471(2001).
7. M.S. Gordon, J.R. Hove, P.W. Webb, and D. Weihs, "Boxfishes as unusually well controlled autonomous underwater vehicles," *Physiol. Biochem. Zool.*, **73**, 663-671 (2001).
8. I.K. Bartol, M. Gharib, P.W. Webb, D. Weihs, and M.S. Gordon, "Body-induced vortical flows: a common mechanism for self-corrective trimming control in boxfishes," *J. Exp. Biol.*, **208**, 327-344 (2005).
9. L. Besseau and Y. Bouligand, "The twisted collagen network of the box-fish scutes," *Tiss. & Cell*, **30**, 251-260 (1998).
10. W. Blake, "Ostraciiform locomotion," *J. Mar. Biol. Assoc. UK*, **57**, 1047-1055 (1977).
11. M.S.K Khan, MAM Siddique, MA Haque, "New record of the longhorn cowfish *Lactoria cornuta* (Linnaeus 1758) from inshore waters of the Bay of Bengal, Bangladesh," *Zool. and Ecol.*, **23**, 88-90 (2013).
12. T. Ikoma, H. Kobayahi, J. Tanaka, D. Walsh, S. Mann, "Microstructure, mechanical, and biomimetic properties of fish scales from *Pagrus major*," *J. Struct. Biol.*, **142**, 327-333 (2003).
13. W. Yang, B. Gludovatz, E.A. Zimmermann, H.A. Bale, R.O. Ritchie and M.A. Meyers, "Structure and fracture resistance of alligator gar (*Atractosteus spatula*) armored fish scales," *Acta Biomater.*, **9**, 5876-5889 (2013).

14. S. Weiner, W. Traub, H.D. Wagner, "Lamellar bone: structure-function relationships," *J. Struct. Biol.*, **126**, 241-255 (1999).
15. A.B. Castro-Ceseña, E. Novitskaya, P.-Y. Chen, M. del Pilar Sánchez-Saavedra, G. Hirata, and J. McKittrick, "Comparison of demineralized and deproteinized bone," *Mater. Res. Soc. Symp. Proc.*, **1301**, 2011, doi: 10.1557/opl.2011.194.
16. W. Yang, J. McKittrick, "Separating the influence of the cortex and foam on the mechanical properties of porcupine quills," *Acta Biomater.*, 2013 (in press), doi: 10.1016/j.actbio.2013.07.004
17. A. Miserez, J.C. Weaver, P.B. Pedersen, T. Schneeberk, R.T. Hanlon, D. Kisailus, H. Birkedal, "Microstructural and biochemical characterization of the nanoporous sucker rings from *Dosidicus gigas*," *Adv. Mater.*, **21**, 401-406 (2009).
18. Z. Manilay, E. Novitskaya, E. Sadovnikov, J. McKittrick, "A comparative study of mature and young cortical bone," *Acta Biomater.*, **9**, 5280-5288 (2013).
19. J.D. Currey, "Mechanical properties of bone tissues with greatly differing functions," *J. Biomech.*, **12**, 313-319 (1979).